GaN Nanowire Arrays for High-Output Nanogenerators

Chi-Te Huang,[†,‡] Jinhui Song,[†] Wei-Fan Lee,[‡] Yong Ding,[†] Zhiyuan Gao,[†]
Yue Hao,[§] Lih-Juann Chen,[*,‡] and Zhong Lin Wang[†,*]

*School of Materials Science and Engineering, Georgia Institute of Technology, Atlanta,
Georgia 30332, Department of Materials Science and Engineering, National Tsing-Hua
University, Hsin-Chu, Taiwan 30013, Republic of China, and Microelectronics Institute, Xidian
University, Xi'an 710071, China*

Received November 20, 2009; E-mail: zhong.wang@mse.gatech.edu; ljchen@mx.nthu.edu.tw

Abstract: Three-fold symmetrically distributed GaN nanowire (NW) arrays have been epitaxially grown on GaN/sapphire substrates. The GaN NW possesses a triangular cross section enclosed by $(000\bar{1})$, $(2\bar{1}\bar{1}2)$, and $(\bar{2}112)$ planes, and the angle between the GaN NW and the substrate surface is ∼62°. The GaN NW arrays produce negative output voltage pulses when scanned by a conductive atomic force microscope in contact mode. The average of piezoelectric output voltage was about −20 mV, while 5−10% of the NWs had piezoelectric output voltages exceeding −(0.15−0.35) V. The GaN NW arrays are highly stable and highly tolerate to moisture in the atmosphere. The GaN NW arrays demonstrate an outstanding potential to be utilized for piezoelectric energy generation with a performance probably better than that of ZnO NWs.

Introduction

Energy is the fundamental deciding factor for the sustainable development of human civilization.[1] Although our current energy relies on fossil fuels, searching for nanoenabled sustainable green energy is one of the utmost important fields of today's research, which includes but is not limited to solar cells,[2−6] thermoelectric modules,[7] and hydrogen fuel cells.[8,9] It has been traditionally believed that mechanical energy may not be significant enough for solving the world energy needs, but such energy exists almost everywhere and at all times. Mechanical energy has been proposed as a potential energy source for powering small electronic components. Recently, using the unique semiconducting and piezoelectric properties, wurtzite-structured materials, such as ZnO,[10−13,15−17] GaN, CdS,[14] and ZnS,[15] have been demonstrated as great candidates for piezo-electric nanogenerators that convert mechanical energy into electricity. The nanogenerator is a transient flow of current in the external load as driven by the piezoelectric potential (e.g., piezopotential) created by dynamic straining in the nanowires.

GaN is well-known for its excellent optoelectronic properties with direct and wide bandgap, high mobility, and excellent thermal stability.[18,19] For improving the performance and efficiency, GaN nanowire (NW) arrays are promising building blocks for future applications of nanodevices with excellent performance, such as laser,[20,21] LED,[22,23] and solar cells.[24] Moreover, the piezoelectric and semiconducting properties of GaN NW arrays could be further utilized for the applications of the piezoelectric nanogenerator to extract energy from environment. But the growth of GaN NWs is possible only via a vapor-phase deposition process. For the epitaxial growth of GaN NW arrays, the substrates play an important role in determining the epitaxial relationship between the GaN NW and the substrate. So far, Si,[24,25,27] GaN,[26] sapphire,[22,23,27,28] MgO,

[†] Georgia Institute of Technology.
[‡] National Tsing-Hua University.
[§] Xidian University.

(1) Wang, Z. L. *Adv. Funct. Mater.* **2008**, *18*, 1.
(2) Huynh, W. U.; Dittmer, J. J.; Alivisatos, A. P. *Science* **2002**, *295*, 2425.
(3) Dresselhaus, M. S.; Thomas, I. L. *Nature* **2001**, *414*, 332.
(4) Weintraub, B.; Wei, Y.; Wang, Z. L. *Angew. Chem., Int. Ed.* **2009**, *48*, 1.
(5) Law, M.; Greene, L. E.; Johnson, J. C.; Saykally, R.; Yang, P. *Nat. Mater.* **2005**, *4*, 455.
(6) Tian, B.; Zheng, X.; Kempa, T. J.; Fang, Y.; Yu, N.; Yu, G.; Huang, J.; Lieber, C. M. *Nature* **2007**, *449*, 885.
(7) Boukai, A. I.; Bunimovich, Y.; Tahir-Kheli, J.; Yu, J. K.; Goddard, W. A.; Heath, J. R. *Nature* **2008**, *451*, 168.
(8) Schlapbach, L. *Nature* **2009**, *460*, 809.
(9) Steele, B. C. H.; Heinzel, A. *Nature* **2001**, *414*, 345.
(10) Wang, Z. L.; Song, J. *Science* **2006**, *312*, 242.
(11) Wang, X.; Song, J.; Liu, J.; Wang, Z. L. *Science* **2007**, *316*, 102.
(12) Xu, S.; Wei, Y.; Liu, J.; Yang, R.; Wang, Z. L. *Nano Lett.* **2008**, *8*, 4027.
(13) Lu, M. P.; Song, J.; Lu, M. Y.; Chen, M. T.; Gao, Y.; Chen, L. J.; Wang, Z. L. *Nano Lett.* **2009**, *9*, 1223.
(14) Lin, Y. F.; Song, J.; Ding, Y.; Lu, S. Y.; Wang, Z. L. *Appl. Phys. Lett.* **2008**, *92*, 022105.
(15) Lu, M. Y.; Song, J.; Lu, M. P.; Lee, C. Y.; Chen, L. J.; Wang, Z. L. *ACS Nano* **2009**, *3*, 357.
(16) Yang, R.; Qin, Y.; Dai, L.; Wang, Z. L. *Nature Nanotechnol.* **2009**, *4*, 34.
(17) Yang, R.; Qin, Y.; Li, C.; Zhu, G.; Wang, Z. L. *Nano Lett.* **2009**, *9*, 1201.
(18) Huang, Y.; Duan, X.; Cui, Y.; Lieber, C. M. *Nano Lett.* **2002**, *2*, 101.
(19) Kuykendall, T.; Pauzauskie, P.; Lee, S.; Zhang, Y.; Goldberger, J.; Yang, P. *Nano Lett.* **2003**, *3*, 1063.
(20) Qian, F.; Li, Y.; Gradecak, S.; Park, H. G.; Dong, Y.; Ding, Y.; Wang, Z. L.; Lieber, C. M. *Nat. Mater.* **2008**, *7*, 701.
(21) Johnson, J. C.; Choi, H. J.; Knutsen, K. P.; Schaller, R. D.; Yang, P.; Saykally, R. J. *Nat. Mater.* **2002**, *1*, 106.
(22) Zhong, Z.; Qian, F.; Wang, D.; Lieber, C. M. *Nano Lett.* **2003**, *3*, 343.
(23) Kim, H. M.; Cho, Y. H.; Lee, H.; Kim, S. I.; Ryu, S. R.; Kim, D. Y.; Kang, T. W.; Chung, K. S. *Nano Lett.* **2004**, *4*, 1059.
(24) Tang, Y. B.; Chen, Z. H.; Song, H. S.; Lee, C. S.; Cong, H. T.; Cheng, H. M.; Zhang, W. J.; Bello, I.; Lee, S. T. *Nano Lett.* **2008**, *8*, 4191.
(25) Calarco, R.; Meijers, R. J.; Debnath, R. K.; Stoica, T.; Sutter, E.; Luth, H. *Nano Lett.* **2007**, *7*, 2248.

and LiAlO$_2$[29] substrates are usually utilized for the epitaxial growth of GaN NW arrays.

In this study, 3-fold symmetrically distributed GaN NW arrays are epitaxially grown on the GaN/sapphire substrates. The structures of the GaN NWs with triangular cross-section have been fully studied. The nanogenerator output measured using the GaN NWs has shown an output that is higher than that of ZnO NWs, and for some NWs, the output voltage of a single NW is as high as -(0.15−0.35) V. Our results not only fully support the mechanism previously proposed for the ZnO NW based piezoelectric nanogenerator but also demonstrate that GaN NWs are a promising candidate for high output nanogenerators.

Experimental Methods

The growth was based on a vapor−liquid−solid process. For substrate preparation, 2-μm-thick wurtzite structured (0001) GaN film was grown epitaxially on the 2-in. (0001) sapphire wafers (c-plane) by MOCVD. A 2−5-nm thin film of Ni was deposited onto GaN-coated sapphire wafers at about 10^{-5} torr in a magnetron RF sputter system at a rate of 0.1 nm s^{-1}. The Ni thin film served as the catalyst for the growth of GaN NW arrays. GaN NW arrays were synthesized via thermal evaporation and condensation processes in a horizontal tube furnace, composed of an alumina tube, a mechanical pump system, and a gas supply and control system. Gallium metal and GaN powder were used as Ga source. Ammonia gas (NH$_3$) was used as carrier gas and served as the N source for the growth of GaN NWs. The mixed Ga metal and GaN powder at a weight ratio of 1:1 was located in the center of the furnace, and the substrate was placed downstream for the growth and collection of GaN NW arrays. Then, the alumina tube was evacuated to a pressure below 8×10^{-3} torr for several hours to vent the residual oxygen and moisture. After keeping the pressure of the system below 8×10^{-3} torr for several hours, the furnace system was heated to 1000 °C at a heating rate of 30 °C min^{-1} under a NH$_3$ flow of 30 sccm (standard cubic centimeters per minute). After the furnace system was kept at 1000 °C for 60 min, it was allowed to cool to room temperature. The morphology, crystal structures, and chemical compositions of samples were characterized and analyzed using scanning electron microscopy (SEM) (LEO 1530 and LEO 1550), X-ray diffraction (XRD) (PRO Alpha-1), and transmission electron microscopy (TEM) (JEOL 4000EX and JEOL JEM-2010).

Results and Discussion

1. Structure of the GaN Nanowires. SEM images of the as-synthesized GaN NW arrays are shown in Figure 1a,b. Top-view SEM images show an overview of high-density and ordered GaN NW arrays on the substrate. The growth directions of the GaN NWs show a 3-fold symmetry as viewed in the image. The diameters and length of GaN NWs range from 25 to 70 nm and 10 to 20 μm, respectively. Longer or shorter NWs could be achieved by varying the growth time. The GaN NW arrays are highly stable and highly tolerant to moisture in the atmosphere, showing no morphological changes over several months when stored in air. The top-view SEM image of a single GaN NW, dispersed on the surface of a silicon substrate, is shown in Figure 1c. The GaN NW possesses a faceted surface and is enclosed by three sidewalls. XRD analysis from an as-grown sample is used to examine the crystal structures of GaN NW arrays, and the spectrum is shown in Figure 1d. There are
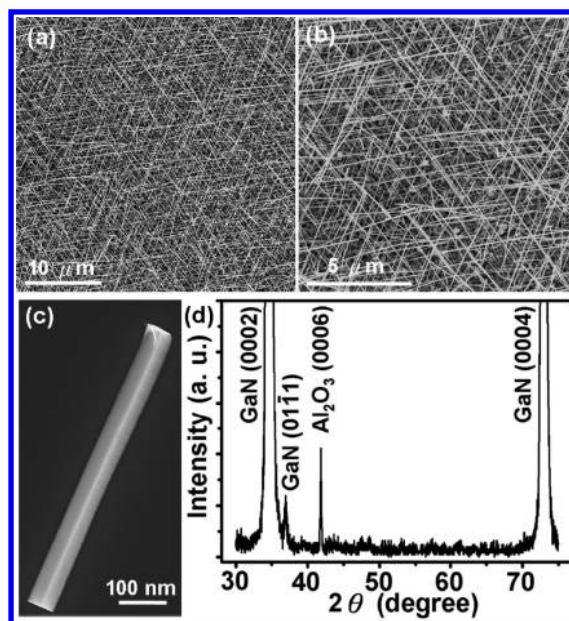
(26) Hersee, S. D.; Sun, X.; Wang, X. *Nano Lett.* **2006**, *6*, 1808.
(27) Kim, H. M.; Kim, D. S.; Park, Y. S.; Kim, D. Y.; Kang, T. W.; Chung, K. S. *Adv. Mater.* **2002**, *14*, 991.
(28) Yoo, J.; Hong, Y. J.; An, S. J.; Yi, G. C.; Chon, B.; Joo, T.; Kim, J. W.; Lee, J. S. *Appl. Phys. Lett.* **2006**, *89*, 043124.
(29) Kuykendall, T.; Pauzauskie, P. J.; Zhang, Y.; Goldberger, J.; Sirbuly, D.; Denlinger, J.; Yang, P. *Nat. Mater.* **2004**, *3*, 524.
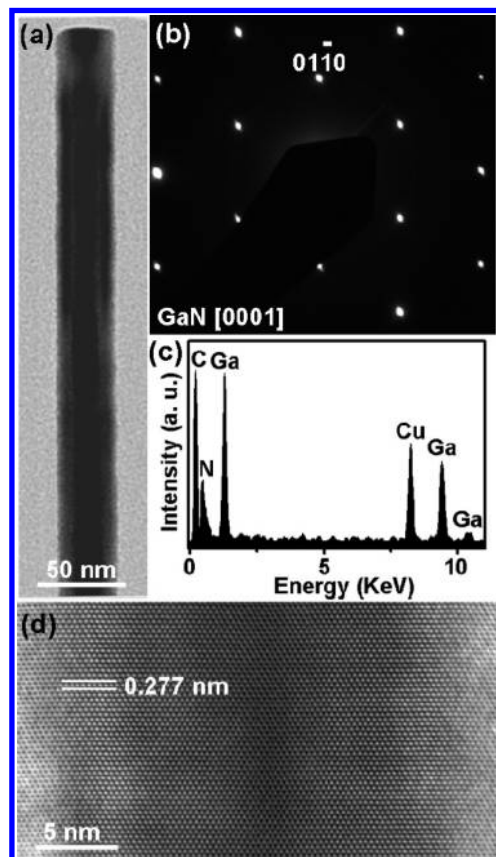
Figure 1. Morphological characterization of GaN NW arrays and crystallographic relationship between GaN NW arrays and GaN/sapphire substrate. (a, b) Low-magnification and high-magnification SEM images of 3-fold symmetrically distributed GaN NW arrays epitaxially grown on GaN/sapphire substrate. (c) Top-view SEM image of a single GaN NW with a triangular cross section. (d) XRD spectrum of GaN NW arrays indicating the epitaxial relationship between GaN NW arrays and GaN/sapphire substrate.

three sets of XRD peaks appearing in the XRD spectrum. Two sets of peaks are attributed to the substrates used for the growth and collection of GaN NW arrays. Considerably stronger peaks corresponding to the (0002) plane of wurtzite-structured GaN with lattice constants of $a = 0.3189$ nm and $c = 0.5185$ nm and a (0001) plane of Al$_2$O$_3$ reveal the epitaxial relationship between the GaN film and c-plane sapphire wafer. The other set of peaks comes from the GaN NW arrays. The spectrum shows exclusively one wurtzite-structured GaN (01$\bar{1}$1) peak. The epitaxial relationship between GaN NW arrays and the GaN films could be further identified as the (01$\bar{1}$1) plane of GaN NW arrays is parallel to the (0001) plane of the GaN substrate film.

The nanostructures of GaN NWs were characterized using TEM. The TEM analyses, including the low-magnification TEM images, high-resolution TEM (HRTEM) images, selected-area electron diffraction (SAED), and energy-dispersive X-ray spectroscopy (EDS), demonstrate the detailed crystal structures and compositions of GaN NWs. Figure 2a shows a low-magnification TEM image of a GaN NW. The diameter of this GaN NW is about 45 nm, which is very uniform along the growth direction. The corresponding SAED and HRTEM images are shown in parts b and d, respectively, of Figure 2. The corresponding SAED along the wurtzite-structured GaN [0001] axis indicates that the growth direction of the NW is along [01$\bar{1}$0]. The lattice fringes from the HRTEM image clearly illustrate that the GaN NW possesses high-quality single-crystal structure without dislocations. The lattice fringes perpendicular to the growth direction are separated by about 0.277 nm, corresponding to the (01$\bar{1}$0) plane of wurtzite-structured GaN, indicating its growth direction of [01$\bar{1}$0]. In addition, the GaN NWs possess clean surfaces without any adhered particles or contamination. The EDS spectrum, shown in Figure 2c, indicates the presence of Ga, N, C, and Cu elements, where the C and

Figure 2. Crystal structures and compositions of GaN NW. (a) Low-magnification TEM image of GaN NW. (b) Corresponding SAED of GaN NW with [0001] zone axis. The growth direction of GaN NW is along the [01$\bar{1}$0]. (c) Corresponding EDS spectra acquired from GaN NW. (d) Atomic resolution TEM image of GaN NW taken along the [0001] zone axis.

Cu peaks come from Cu grid covered with C film. The result indicates that the NWs are composed of Ga and N elements, just as expected.

Figure 3a show a 30° tilt view SEM image of a GaN NW. The GaN NW could be clearly observed to possess a triangular cross section with about 70 nm at its base. The cross-sectional TEM analysis has been used to understand the detailed crystal structure and facets of the GaN NWs. The TEM image and corresponding SAED are shown in parts b and c of Figure 3. The TEM image reveals the triangular cross section of the GaN NW, and its base is about 70 nm. The internal angles of the triangular cross section are measured to be about 58°, 58.5°, and 64°. The corresponding SAED is along the wurtzite-structured GaN [01$\bar{1}$0] axis. Moreover, this [01$\bar{1}$0] zone axis is parallel to the growth direction of GaN NWs. By indexing the SAED pattern, three facets enclosing the GaN NW could be identified as (000$\bar{1}$), (2$\bar{1}$$\bar{1}$2), and ($\bar{2}$112) planes. The standard internal angles of the triangular cross section enclosed by the three planes are calculated to be 58.42°, 58.42°, and 63.16°, in good agreement with the measured values. The result means that the cross section of a GaN NW would be an isosceles rather than an equilateral triangle.[19] The measured internal angles, TEM image, and SAED results consistently prove the crystal structure and facets of the GaN NWs with a triangular cross section.

The model shown in Figure 3d exhibits the crystallographic relationship between a GaN NW and the substrate. The SAED shown in Figure 2b indicates the growth direction of the GaN NW is along [01−10], and the XRD spectrum shown in Figure
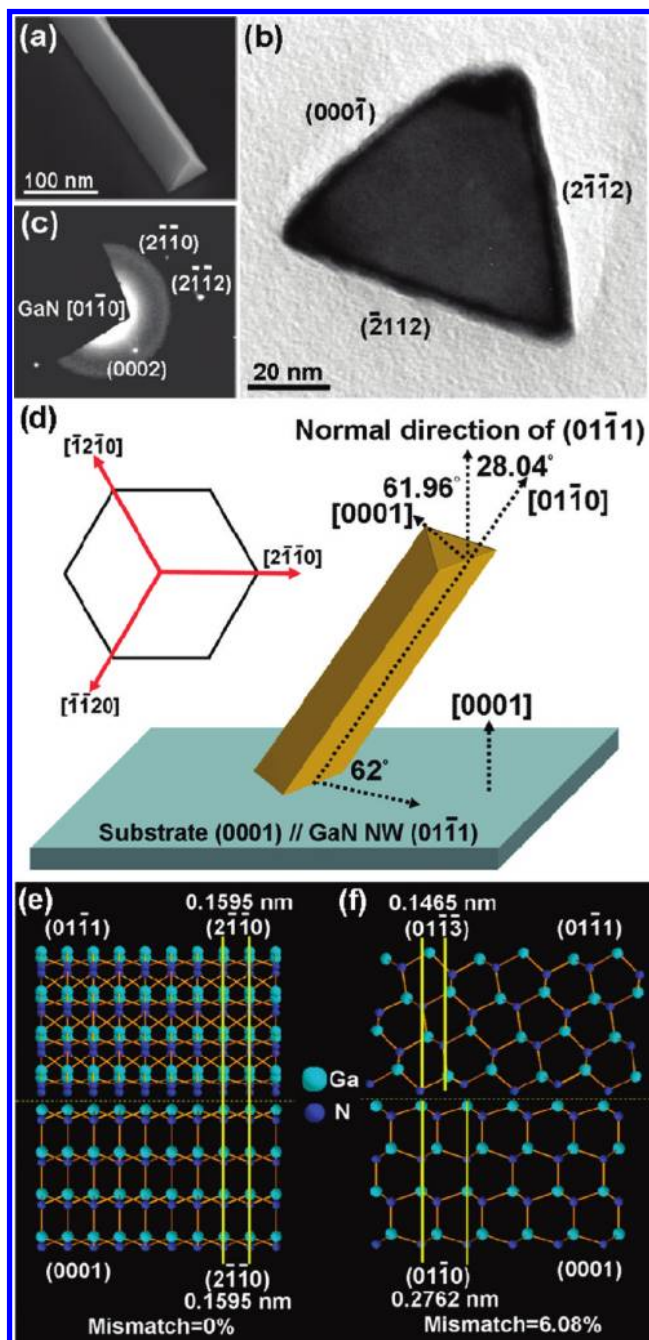

Figure 3. Morphological characterization and crystal structures of GaN NW with a triangular cross section. (a) 30° tilt view SEM image of GaN NW with a triangular cross section. (b) Cross-sectional TEM image of GaN NW enclosed by (000$\bar{1}$), (2$\bar{1}$$\bar{1}$2), and ($\bar{2}$112) planes. (c) Corresponding SAED of GaN NW recorded along the [01$\bar{1}$0] zone axis. (d) Schematic diagram showing crystallographic relationship between GaN NW and GaN/sapphire substrate. The inset is the model for forming the 3-fold symmetric distribution of NWs on the substrate. (e, f) Atomic model exhibiting the epitaxial relationship between GaN NW and GaN/sapphire substrate.

1d indicates the (01$\bar{1}$1) plane of GaN NW arrays is parallel to the (0001) plane of the GaN substrate film. On the basis of SAED and XRD results, the angle between GaN NW and the substrate is calculated to be about 62°. The inset of Figure 3d exhibits the schematic diagram of the GaN NW arrays that exhibit a 3-fold symmetry on the substrate due to the equivalent crystal orientations. To realize the detailed crystallographic relationship between GaN NW arrays and the substrate, we present a crystallographic model to describe the epitaxy of

$(01\bar{1}1)_{NW}$ on $(0001)_{substrate}$. The atomic models of cross section of the NW/substrate interface shown in parts e and f of Figure 3 could clearly display the detailed crystallographic relationship between the GaN NW and the GaN substrate. Figure 2e exhibits the cross section at the interface between the NW at the $[01\bar{1}2]_{NW}$ zone axis and the substrate at the $[01\bar{1}0]_{substrate}$ zone axis. In the perpendicular direction, the cross section of interface between the NW at the direction of the $[2\bar{1}\bar{1}0]_{NW}$ zone axis and the substrate at $[2\bar{1}\bar{1}0]_{substrate}$ zone axis is shown in Figure 2f. The crystallographic relationship of interface is as follows:

$$(01\bar{1}1)_{NW}//(0001)_{substrate}, [2\bar{1}\bar{1}0]_{NW}//[2\bar{1}\bar{1}0]_{substrate}$$

The $(2\bar{1}\bar{1}0)_{NW}$ plane ($d = 0.1595$ nm) perfectly matches the $(2\bar{1}\bar{1}0)_{Substrate}$ plane ($d = 0.1595$ nm), with zero mismatch. In the perpendicular direction, two $(01\bar{1}3)_{NW}$ planes ($d = 0.1465$ nm) match one $(01\bar{1}0)_{substrate}$ plane ($d = 0.2762$ nm), resulting in a mismatch of 6.08%. To understand the growth mechanism of the 3-fold geometric symmetry of the GaN NW arrays, lattice mismatch is known to play a significant role in the epitaxial growth of homogeneous or heterogeneous structures. The interface of the NW/substrate would prefer to take the least mismatch to reduce the interface mismatch energy. The $[2\bar{1}\bar{1}0]$ directions of the $(01-11)_{NW}$ plane matches perfectly with the $[2\bar{1}\bar{1}0]$ directions of the $(0001)_{Substrate}$ plane. Moreover, the $[2\bar{1}\bar{1}0]$ direction of the $(0001)_{substrate}$ plane is a 3-fold symmetry orientation. Based on the above results, we believe that the 3-fold geometric symmetry of GaN NW arrays must be attributed to the excellent match of GaN NWs and substrate along the three $\langle 2\bar{1}\bar{1}0 \rangle$ directions, as shown in the inset in Figure 3d.

2. Piezoelectric Potential in GaN Nanowire. Owing to its piezoelectric property, a piezoelectric potential is created in a GaN NW once it is strained. Although the magnitude of the piezopotential is related to the doping in the NW, a semiquantitative understanding can be obtained by numerical calculation without considering the doping. For simplicity, we assume that a NW is fixed at one end (bottom side) and the other end is pushed by a point force analogous to the action of an atomic force microscope (AFM) tip. The Lippman theory[30] was used to calculate the piezopotential distribution in a bent GaN NW. The length and diameter of the GaN NW was set to be 10 μm and 50 nm, respectively, and the lateral force applied by AFM tip was 80 nN. The material constants of the GaN NW used in the calculations are $a = 0.3189$ nm, $c = 5.185$ nm, $C_{11} = 390$ GP, $C_{12} = 145$ GP, $C_{13} = 106$ GP, $C_{33} = 398$ GP, $C_{44} = 105$ GP, piezoelectric constants $e_{15} = -0.49$ C/m^2, $e_{31} = -0.49$ C/m^2, $e_{33} = 0.73$ C/m^2, relative dielectric constants $\kappa_{11} = \kappa_{12} = \kappa_{\perp} = 9.28$, $\kappa_{33} = \kappa_{\parallel} = 10.01$,[31] and the density $\rho = 6150$ kg/m^3. Owing to the triangular cross-section of the NW, the piezopotential depends on the direction along which the force is applied. The plot shown in Figure 4a exhibits the detailed crystal structure of the GaN NW used for the calculation. The coordinate system shown in Figure 4b reveals the angle between the GaN NW and x-axis is about 62°. The plots of the calculated piezoelectric potential distributions of the GaN NW for the forces being applied along different directions are shown in Figure 4c–f. The color code represents the output potential. The red and blue stand for positive and negative potential,
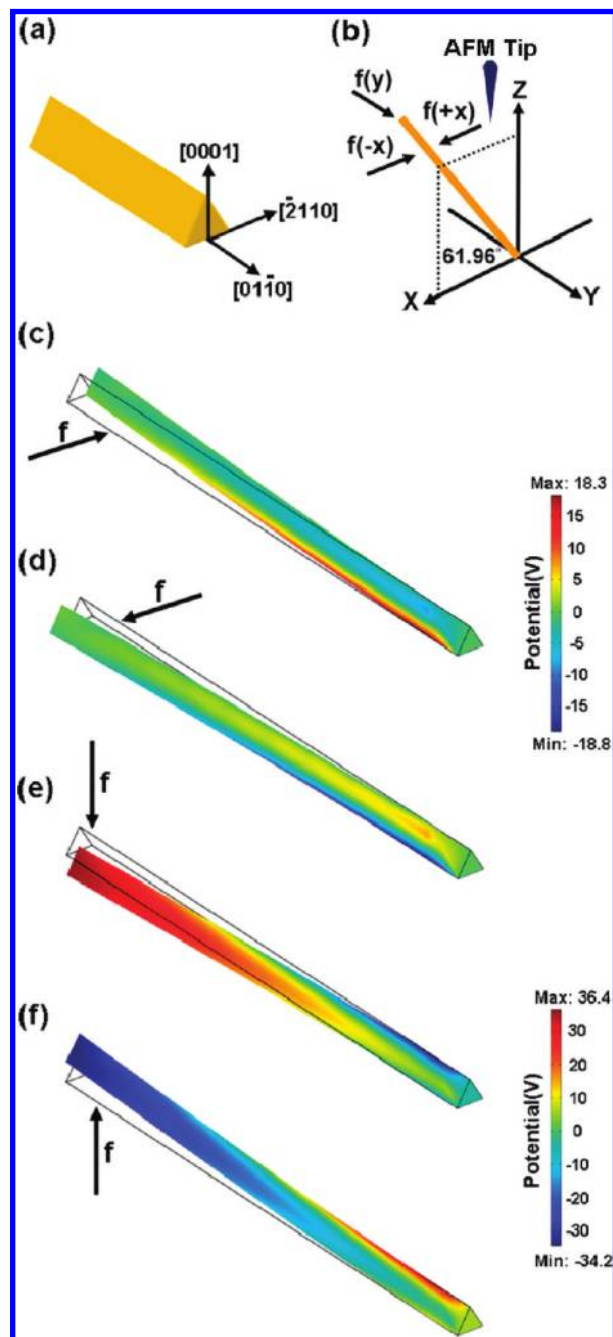
(30) Gao, Y.; Wang, Z. L. *Nano Lett.* **2007**, *7*, 2499.
(31) Fonoberov, V. A.; Balandin, A. A. *J. Appl. Phys.* **2003**, *94*, 7178.
(32) Chang, C. Y.; Chi, G. C.; Wang, W. M.; Chen, L. C.; Chen, K. H.; Ren, F.; Pearton, S. J. *J. Electron. Mater.* **2006**, *35*, 738.

Figure 4. (a) Detailed crystal structure of GaN NW with triangular cross-section utilized for calculation of piezoelectric potential distribution. (b) Coordinate system used to define the direction of lateral force applied from the AFM tip. (c–f) Calculated piezoelectric potential distribution for the GaN NW. The dimension of the NW is the base of NW = 50 nm, length = 10 μm, applied lateral force = 80 nN.

respectively. The coordinate system shown in Figure 4b is also utilized to define the direction of the applied force. For simplicity of the calculation, we assume the GaN NW is bent by the AFM tip in three different ways, along +y, +x, and −x axis directions. In the first case, the GaN NW is bent laterally along the +y direction. The plots shown in Figure 4c,d represent the stretched and compressed sides of the GaN NW, respectively. The GaN NW would produce positive potential at the stretched side and negative potential at the compressed side. However, the piezoelectric potential decreases gradually from the bottom to the top of the NW. In alternative cases, the force is applied to push the NW along the +x or −x axis direction, and the

corresponding piezopotenital distributions are shown in parts e and f, respectively, of Figure 4. The top of the NW produces a positive and negative potential when the NW was pushed by AFM tip along the $+x$ and $-x$ axis directions, respectively.

The above calculated results can be extrapolated to include the effect as a result of doping.[33] The as-grown GaN NW would be an intrinsic n-type semiconductor without any intentional doping.[18,19,32] Based on our previous study,[33,34] the electrons of the n-type GaN NW would accumulate at the positive piezopotenital side (stretched side) to screen the positive piezoelectric potential but leave the negative piezopotential unchanged when the carrier concentration is not too high, which is the acting driving force for control the transport of the carriers. This means that we can ignore the positive piezopotential in our following discussions.

3. Nanogenerator Using GaN Nanowires. We now follow the method previously demonstrated for using ZnO NWs to convert mechanical energy into electricity.[10,13−15] The piezoelectric measurements of the GaN NW arrays were performed using the AFM (Molecular Force Probe MFP-3D from Asylum Research) in contact mode. The Pt-coated Si tip, tetrahedral shape with a cone angle of 70°, was utilized as the AFM tip, and the spring constant of the cantilever was calibrated to be 3.5 N/m. In the contact mode, a constant normal force of 5 nN was applied between the AFM tip and surface of GaN NW arrays. To ensure the sample was well grounded, silver paste was utilized to connect the GaN film on the substrate surface with the measurement circuit. When the tip scanned across the GaN NW arrays, the output electrical signals were continuously monitored across an external load of resistance $R_L = 500$ MΩ. It should be noted that no external voltage was applied during any period of measurements. Figure 5a exhibits the 3D electric image of output potential peaks generated by GaN NW arrays with a scanning area of 20 μm × 20 μm, and the color code represents the output potential. The AFM tip scans across the sample to laterally bend the GaN NW arrays and the output electric signals were consecutively monitored and recorded across an external load. The plot reveals almost all of the output signals are negative with an average output potential about −20 mV and some output signals could reach a magnitude of several hundred -mV, which are a lot higher than those received for ZnO NWs. Figure 5b shows a 20 μm line profile of output signals. All of the voltage peaks indicated negative potential.

The strain-induced piezoelectric potential would be the key to understanding the physical mechanism of the energy-harvesting process using GaN NW arrays. According to the calculated piezoelectric potential distribution shown in Figure 4, the bent GaN NW would have three different types of piezoelectric potential distributions depending on the direction of the applied force. The plots shown in parts c and d of Figure 4 represent the first case, the stretched and compressed sides of the GaN NW would exhibit positive and negative piezoelectric potential, respectively, and the magnitude of the piezoelectric potential is the maximum toward the bottom of the NW. If we consider the carrier type and conductivity of the n-type GaN NW, the positive piezoelectric potential would be largely screened by electrons.[33,34] As for the case shown in Figure 4c,d, the piezoelectric output is expected to be small. This case may be responsible for the smaller output voltage peaks from the nanogenerator.
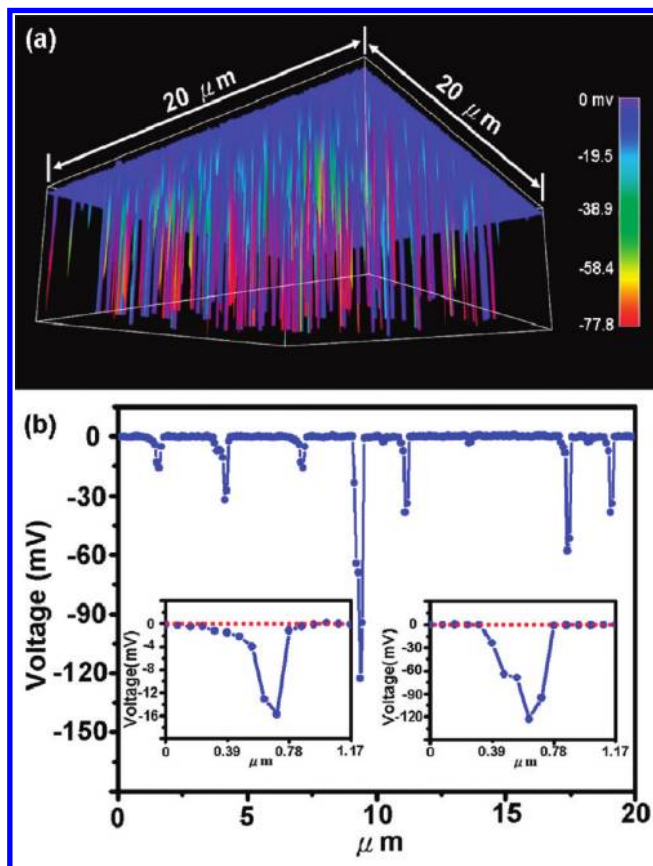
(33) Gao, Y.; Wang, Z. L. *Nano Lett.* **2009**, *9*, 1103.

Figure 5. Piezoelectric power generation using the GaN NW arrays. (a) Three-dimensional plot of the output voltage recorded at an external load when the AFM tip scanned and deflected the NW arrays. (b) A typical line scan profile of the output voltage. Insets show the detailed line profile of individual output peaks with high and low output voltages.
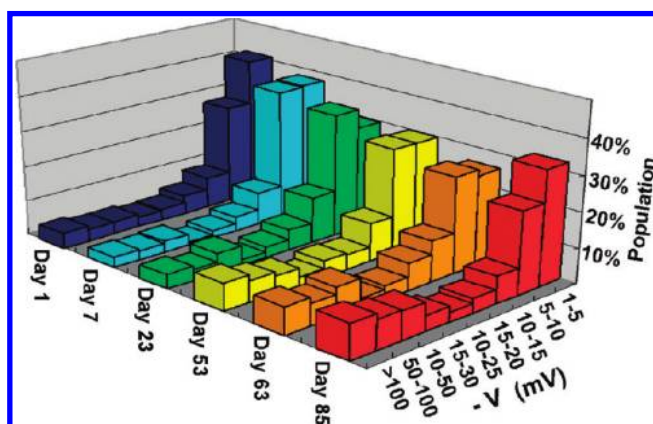

Figure 6. Statistical distribution of the piezoelectric output measured from the same GaN NW arrays sample as a function of time to test the stability and reproducibility.

The case shown in Figure 4f is likely to be the dominant piezoelectric output. When the screening effect of the n-type carriers in the GaN NWs is considered, the positive piezopotential is largely screened; thus, it will not be effective for driving the carriers. The large negative piezopotential observed experimentally is likely due to the potential distribution shown in Figure 4f. We must notice that the explanation of the details of the piezopotential output needs to consider the shape of the nanowire and the shape of the AFM tip. With considering the triangular cross-section of the nanowire and its inclined orientation on the substrate as well as the pyramid

shape of the tip, bending and twist of the nanowire is possible when the tip contacts the nanowire; thus, the distribution of the piezo-potential in the nanowire is more complex than those shown in Figure 4.[35] Therefore, caution has to be taken when apply the model developed for a cylindrical symmetric, vertically aligned nanowire.

To examine the stability and reproducibility of the piezoelectric output generated by GaN NW arrays, we have utilized the same sample for all of the measurements during 3 months. The chart shown in Figure 6 presents the statistical distribution of the output voltage generated by the GaN NW arrays. Because the area used for measurements would change, the density, morphology, and aspect ratio of GaN NWs would have little variation. The distributions between each measurement would have little variations, but the majority of output voltages are within the range from -1 to -10 mV. About $30-50\%$ of output voltages exceed -10 mV, and $5\%-10\%$ of output voltages could reach the magnitude of several hundred -mV. The result reveals that the GaN NWs exhibit good stability and performance in the application of piezoelectric nanogenerator. This result is very consistent with the SEM observation. The GaN NW arrays showed no morphological change over several months when stored in air.

Conclusions

In summary, we have successfully synthesized the 3-fold symmetrically distributed GaN NW arrays, grown epitaxially on the GaN/sapphire substrates. The crystallographic relationship between the GaN NW and substrate is $(01\bar{1}1)_{NW}$// $(0001)_{substrate}$, $[2\bar{1}\bar{1}0]_{NW}$//$[2\bar{1}\bar{1}0]_{substrate}$. The TEM and XRD results indicate that the GaN NW possesses a triangular cross section enclosed by $(000\bar{1})$, $(2\bar{1}\bar{1}2)$, and $(\bar{2}112)$ planes, and the angle between the GaN NW and the substrate surface is about $62°$. The n-type GaN NW arrays produce negative piezoelectric output voltage. The average of piezoelectric output voltage was about -20 mV, while $5-10\%$ of the NWs had piezoelectric output voltages exceeding -100 mV. The SEM result illustrates that the GaN NW arrays are highly stable, showing no morphological changes over several months when stored in air. The result is consistent with the statistic results of piezoelectric output voltage distributions. The distributions of piezoelectric output voltage generated by GaN NW arrays are quite stable during the experiment period of three months. On the basis of the above results, the GaN NW arrays show an outstanding potential to be utilized for piezoelectric energy generation with a performance probably better than ZnO NWs.

(34) Mantini, G.; Gao, Y.; D'Amico, A.; Falconi, C.; Wang, Z. L. *Nano Res* **2009**, *2*, 624.
(35) Gao, Z. Y.; Zhou, J.; Gu, Y. D.; Fei, P.; Hao, Y.; Bao, G.; Wang, Z. L. *J. Appl. Phys.* **2009**, *105*, 113707.